

COMPLEX-PLANE CHARTS FOR OBTAINING CLOSED-LOOP FREQUENCY RESPONSES IN LINEAR CONTROL SYSTEMS

By

F. CSÁKI

Department for Special Electrical Machines and Automation,
Polytechnical University, Budapest

(Received August 23, 1960)

One of the fundamental objects of the control systems design is the determination of the closed-loop frequency response from the open-loop one. The former, namely, allows, on the one hand, to quickly evaluate the qualitative performance specifications of the control, and, on the other hand, by the aid of its real or imaginary component the time-functions may be obtained, too. Determination of the closed-loop frequency-response theoretically encounters no difficulties, nevertheless, the analytical evaluation is made difficult in practice, because calculations with complex quantities in five-six steps are necessary.

As a consequence of this, several graphical methods have been developed in engineering practice to solve the above mentioned problem. These may be found in the basic works [e. g. 1, 2, 3, 4]. One of the procedures means application of the NICHOLS-charts [1] in connection with the BODE-diagram [5, 1]. The other method is to plot one of the various complex-plane charts in connection with the magnitude-phase curves. Thus, for plotting the NYQUIST, MIKHAILOV, LEONHARD curves [6, 7, 8, 9], in order to obtain the stability criteria, various direct and inverse complex-plane charts may be employed, as shown in details in the fundamental works [1, 2, 3, 4, 10], and to be found as a new possibility also in a paper published recently [11].

Both the methods connected with the attenuation-frequency diagrams and with the magnitude-phase diagrams have certain advantages and disadvantages, and consequently followers and opponents. To avoid vain debates, the present paper does not take a standpoint in this respect, regarding as its task merely to examine systematically, what are the possibilities of plotting complex-plane charts, permitting to determine in a simple way the closed-loop frequency-response on the basis of the open-loop response, in linear systems. (The systematic investigation of the other problem will perhaps be discussed on another occasion.)

1. Statement of the problem

The block diagram of the most simple unity feedback control system is shown in Fig. 1. Denoting by s the complex variable of the Laplace transform, $R(s)$ being the reference input signal, $C(s)$ the controlled output signal and $E(s)$ the error signal. The open-loop transfer function is $G(s)$, while the closed-loop transfer function is

$$\frac{C(s)}{R(s)} = \frac{G(s)}{1 + G(s)} \quad (1)$$

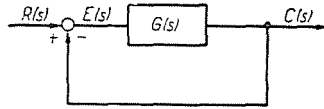


Fig. 1. Unit feedback system block diagram

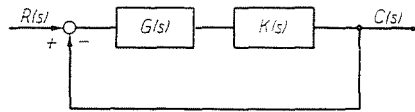


Fig. 2. Block diagram with a series stabilization

If the control system illustrated in Fig. 1 did not meet the control requirements, series, or parallel stabilizing elements are necessary. In the first case (Fig. 2) the open-loop transfer function is $G(s) K(s)$, while the closed-loop one

$$\frac{C(s)}{R(s)} = \frac{G(s) K(s)}{1 + G(s) K(s)} \quad (2)$$

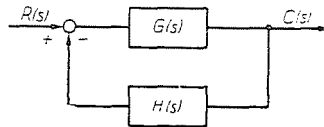


Fig. 3. Parallel stabilization. Block diagram of a general negative feedback system

In the second case (Fig. 3), when applying parallel stabilization, *i. e.* when there is no more unity feedback, the closed-loop transfer function is

$$\frac{C(s)}{R(s)} = \frac{G(s)}{1 + G(s) H(s)} \quad (3)$$

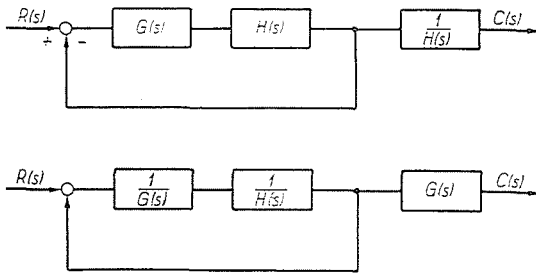
where $G(s)$ means the forward transfer function, while $H(s)$ the feedback transfer function. After some arrangements, relation (3) yields

$$\frac{C(s)}{R(s)} = \left[\frac{G(s) H(s)}{1 + G(s) H(s)} \right] \frac{1}{H(s)} \tag{4a}$$

and

$$\frac{C(s)}{R(s)} = \left[\frac{\frac{1}{G(s) H(s)}}{1 + \frac{1}{G(s) H(s)}} \right] G(s) \tag{4b}$$

Latter relations may be illustrated as shown in Figs. 4a and 4b, respectively.



Figs. 4a and 4b. Tracing back the general negative feedback system to the unit feedback system

Comparing the above relations, it is clear that expressions (2) and (3) are generalizations of expression (1). In spite of this it is evident that if we succeed in elaborating a method for determining the expression (1), this may be applied without more addendum to expression (2), simultaneously facilitating calculation of the transfer function (3) by permitting to adopt it at least to obtain the part of Eqs. (4a) and (4b) in square brackets. After this the whole expression (3) may be determined by a simple division, or multiplication.

Therefore, first of all, the possibilities for solving the problem denoted by expression

$$M(s) = \frac{A(s)}{1 + A(s)} \tag{5}$$

will be dealt with in the following, that is, how and in how many ways the closed-loop transfer function $M(s)$ may be obtained in knowledge of the generalized open-loop transfer function $A(s)$.

2. Symbols

The complex quantities $M(s)$ and $A(s)$ figuring in expression (5), as well as their reciprocals are expressed aided by the following symbols, in canonical, polar and exponential forms:

$$M(s) = U + jV = M \angle \alpha = M e^{j\alpha}$$

$$A(s) = X + jY = A \angle \varphi = A e^{j\varphi}$$

and

$$\frac{1}{M(s)} = N(s) = u + jv = N \angle \beta = N e^{j\beta} \quad (6)$$

$$\frac{1}{A(s)} = B(s) = x + jy = B \angle \psi = B e^{j\psi}$$

where $N = \frac{1}{M}$; $B = \frac{1}{A}$; $\beta = -\alpha$; $\psi = -\varphi$; etc.

3. Possibilities of plotting complex-plane charts

The basic relation (5) may be expressed in the following forms aided by the quantities figuring in Eqs. (6):

$$M(s) = \frac{A(s)}{1 + A(s)} \quad (7)$$

$$M(s) = \frac{1}{1 + B(s)} \quad (8)$$

$$A(s) = \frac{M(s)}{1 - M(s)} \quad (9)$$

$$A(s) = \frac{1}{N(s) - 1} \quad (10)$$

$$B(s) = N(s) - 1 \quad (11)$$

$$B(s) = \frac{1 - M(s)}{M(s)} \quad (12)$$

$$N(s) = 1 + B(s) \quad (13)$$

$$N(s) = \frac{1 + A(s)}{A(s)} \quad (14)$$

Each of the above eight equations (7)...(14) represents a conformal mapping. E.g. by the first Eq. (7) the complex plane $M(s)$ may be mapped onto the complex

reference plane $A(s)$. Let us denote this mapping by the symbol $A(s) [M(s)]$, while the chart arising from it, by the symbol $(A, \varphi, X, Y) [M, a, U, V]$. Latter wants to express that the circles $M = \text{const.}$, further the straight lines of $a = \text{const.}$, $U = \text{const.}$, $V = \text{const.}$ of the plane $M(s)$ appear in the ensemble of the polar co-ordinate system A, φ and of the Cartesian co-ordinate system X, Y of the reference plane $A(s)$ in form of the curves determined by relation (7). In this way on the network A, φ, X, Y the chart determined by the respective set of curves M, a, U, V is originated.

Let us call the chart *complete*, if all the four sets of curves are plotted in the ensemble of the polar and Cartesian co-ordinate systems of the reference plane. If one of the sets of curves is missing, let us term the chart *incomplete*. For example, $(A, \varphi, X, Y) [M, a, U, V]$ determines a complete chart, while $(A, \varphi) [M, a]$ or $(X, Y) [M, a]$ or $(A, \varphi, X, Y) [M, a]$ an incomplete chart within the group of the conformal mapping $A(s) [M(s)]$. Now the question arises, how many kinds of complex-plane charts can be plotted at all?

Evidently, equations (7)...(14) permit only eight complete charts to be plotted, as the eight equations determine eight conformal mapping groups and to each conformal mapping belongs merely one complete chart ($8 \cdot 1^2 = 8$).

The number of the incomplete charts is much higher. The complex variable is perfectly determined by two data, *e. g.* solely by its polar, or by its canonical form, consequently, within the conformal mapping group $A(s) [M(s)]$ the following four incomplete charts are possible: $(A, \varphi) [M, a]$; $(X, Y) [M, a]$; $(A, \varphi) [U, V]$; $(X, Y) [U, V]$. In accordance with the eight mapping groups, altogether *thirty-two* such incomplete charts may be realized ($8 \cdot 2^2 = 32$).

Aside from the above limitation, even higher numbers are obtained. Choosing arbitrary k data from the possible 4 co-ordinate components, this may be realized in $\binom{4}{k}$ manners. Therefore, restricting ourselves to two data as a minimum, considering all of the eight mapping groups together

$$8 \left[\binom{4}{4} + \binom{4}{3} + \binom{4}{2} \right]^2 = 8 (1 + 4 + 6)^2 = 968$$

while restricting ourselves to one mapped component as a minimum, totally

$$8 \left[\binom{4}{4} + \binom{4}{3} + \binom{4}{2} + \binom{4}{1} \right] \left[\binom{4}{4} + \binom{4}{3} + \binom{4}{2} \right] = 8 \cdot 15 \cdot 11 = 1320$$

possibilities open for plotting complex-plane charts. These are unexpectedly high numbers!

4. Some preliminary remarks

In any case, the above discussion convinces us of being more practicable to restrict ourselves, for the sake of a better perspicuity, to the conformal mapping groups instead of the possible charts, as the number of the cases is

at the most eight. In other words, only the complete charts will be discussed and thereby all of the incomplete charts are involved. Nevertheless, the method suggested does not mean an obligation to employ always and in all cases the complete charts. On the contrary, in some cases, if only because of a better perspicuity, neglectation of some sets of curves may seem advantageous, applying incomplete charts.

And now the question arises, what kind of informations should be offered by the plotted charts? First of all it must enlighten, if the closed-loop system is stable, or not, and to decide the stability, criteria must be furnished. (For example, on the basis of the course of curve $A(j\omega)$ or $B(j\omega)$ relative to point -1 , or the mapping of curve $A(j\omega)$ or $B(j\omega)$ with respect to the mapping of point -1 .) Moreover, it has to permit determination of the phase margin and gain margin, which are well-known notions generally applied in control engineering. (The first may be read from the intersection of $A(j\omega)$ and $B(j\omega)$, respectively, and of the unit circle, or from the mappings of both, while the second by the aid of the intersection of $A(j\omega)$ and $B(j\omega)$ respectively, and of the line determined by points 0 and -1 or on the basis of their mappings.) It has to be allowed to obtain the peak magnitude on the closed-loop frequency response curve $M(j\omega)$ (to settle the rough criterion $M_p < 1.4$ or $M_p < 1.3$), as well as to estimate the bandwidth (based on the frequency ω belonging to the intersection of the curves $M = 0.707$ and $M(j\omega)$ or their mappings) and so on.

It is to be emphasized that the above-mentioned stability and qualitative informations *may be obtained from all charts*, for the sake of brevity, however, full details regarding the individual charts will not be given, assuming the application of the above rules in an according sense, and only the possibilities of the readings will be referred to briefly.

After satisfying the stability criteria and meeting the rough design specifications, the claim to determine the transient time-function arises, too. For that purpose the method of FLOYD [2] and of SOLODOVNIKOV [10, 12] may be applied. In case of *unit step* input signal the time function of the output signal may be determined by expressions

$$m(t) = \frac{2}{\pi} \int_0^{\infty} \frac{U(\omega)}{\omega} \sin t\omega \cdot d\omega \quad (15a)$$

or

$$m(t) = \frac{2}{\pi} \int_0^{\infty} \frac{V(\omega)}{\omega} \cos t\omega \cdot d\omega + M(0) \quad (15b)$$

Similarly, in case of *unit impulse* input signal, the time function of the output signal may be expressed by

$$m'(t) = \frac{2}{\pi} \int_0^{\infty} U(\omega) \cos t \omega \cdot d \omega \tag{16a}$$

or

$$m'(t) = - \frac{2}{\pi} \int_0^{\infty} V(\omega) \sin t \omega \cdot d \omega \tag{16b}$$

Consequently, to apply the formulae, the real component $U(\omega)$ or the imaginary one $V(\omega)$ of the closed-loop frequency response $M(j \omega)$ must be known in function of the frequency. Thus the charts directly providing the co-ordinates U and/or V must be regarded as being advantageous, though it must be noted that knowing M and a , determination of the latter encounters no difficulties ($U = M \cos a$ and $V = M \sin a$), so reading M and a is perhaps sufficient.

Before introducing the complete charts, another general remark must be made. All of the conformal mappings given by Eqs. (7)...(14) belong to the well-known conformal mapping class

$$w(s) = \frac{a z(s) + b}{c z(s) + d} \qquad a d - b c \neq 0 \tag{17}$$

determined by the linear fractional transformation. As is known, this mapping is, on the one hand, a one-to-one transform and, on the other hand, it transforms circles onto circles (regarding the straight line as a circle of infinite radius). All of the mapped curves are consequently straights or circles, so their construction is relatively simple. Just this is the great advantage of the complex-plane charts.

5. The eight conformal mappings and the eight complete charts

Now we are going to discuss one after the other the conformal mappings determined by Eqs. (7)...(14) and plotting also the complete charts, restricting ourselves to the range around the origin. The following formulae, of course, permit an arbitrary extension of the figures and the construction of intermediate curves, if necessary.

5.1. Mapping of the closed-loop plane $M(s)$ onto the open-loop plane $A(s)$

The mapping $A(s)$ [$M(s)$] is determined by Eq. (7). For plotting the complete chart (A, φ, X, Y) [M, a, U, V] following equations serve (besides

the polar A, φ and Cartesian X, Y co-ordinate system being in the reference plane):

$$\left[(X+1) + \frac{1}{2(U-1)} \right]^2 + Y^2 = \left[\frac{1}{2(U-1)} \right]^2 \quad (7a)$$

$$(X+1)^2 + \left(Y - \frac{1}{2V} \right)^2 = \left(\frac{1}{2V} \right)^2 \quad (7b)$$

$$\left(X + \frac{M^2}{M^2-1} \right)^2 + Y^2 = \left(\frac{M}{M^2-1} \right)^2 \quad (7c)$$

$$\left(X + \frac{1}{2} \right)^2 + \left(Y - \frac{1}{2 \operatorname{tg} a} \right)^2 = \left(\sqrt{\frac{1}{4} + \frac{1}{4 \operatorname{tg}^2 a}} \right)^2 \quad (7d)$$

The above relations may be obtained from Eq. (7) as follows: On the one hand

$$M(s) = \frac{A(s)}{1+A(s)} = \frac{X+jY}{1+X+jY} = \frac{X^2+X+Y^2+jY}{(1+X)^2+Y^2}$$

On the other hand, considering Eq.(6):

$$U = \frac{X^2+X+Y^2}{(1+X)^2+Y^2} \quad M = \sqrt{\frac{X^2+Y^2}{(1+X)^2+Y^2}}$$

$$V = \frac{Y}{(1+X)^2+Y^2} \quad \operatorname{tg} a = \frac{Y}{X^2+X+Y^2}$$

Latter relations yield consecutively the expressions (7a)...(7d) after some algebraic arrangements. (The formulae of the further cases may be obtained by similar derivations!).

It must be noted that the general form of equations (7a)...(7d) is

$$(X - \xi)^2 + (Y - \eta)^2 = \rho^2$$

the centre of the circles being determined by point $\xi + j\eta$, their radius, however, by ρ .

The complete chart $(A, \varphi, X, Y) [M, a, U, V]$ is shown in Fig. 5. This method of representation is the most widespread one, among the incomplete charts the type $(X, Y) [M, a]$ or $(X, Y) [M]$ and $(X, Y) [a]$ [e. g. 3] and the type $(A, \varphi) [M, a]$ or $(A, \varphi) [M]$ and $(A, \varphi) [a]$ [e. g. 2] are the most common ones.

The stability can be decided on the basis of the well-known NYQUIST criterion. The gain margin and the phase margin can easily be read. The peak M_p and the bandwidth can be obtained by the aid of the curves $M = \text{const.}$

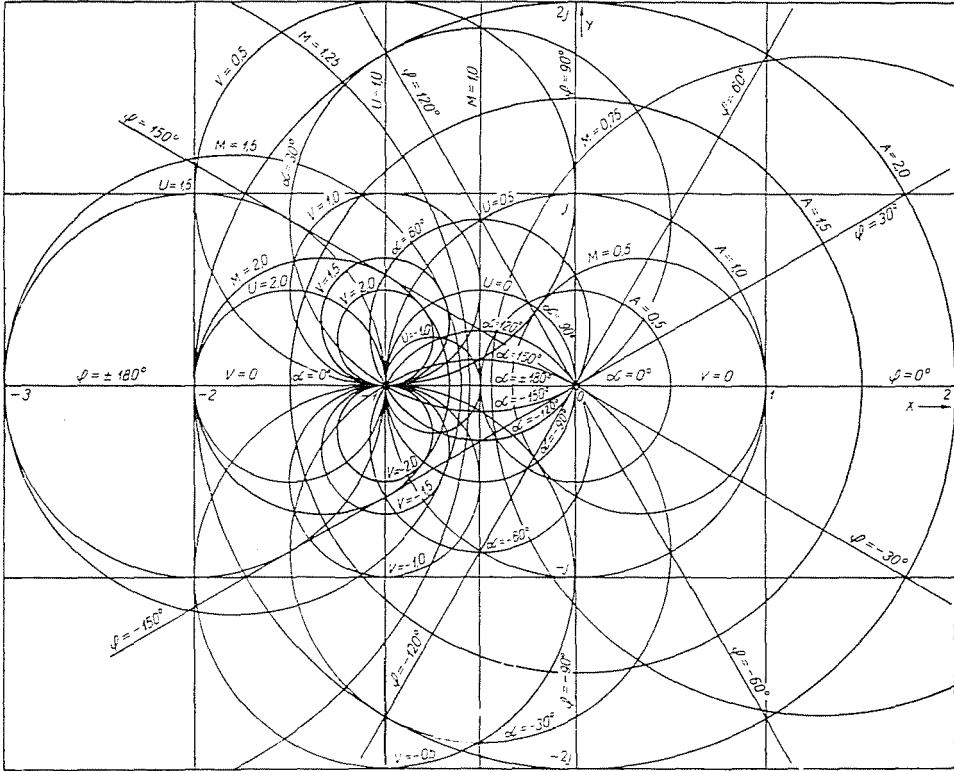


Fig. 5. Mapping of plane $M(s)$ onto the reference plane $A(s)$. Chart $(A, \varphi, X, Y) [M, a, U, V]$

Disadvantage of this method is that reading $M, a, U,$ and V is somewhat cumbersome. The direct performance of the division and multiplication, respectively, corresponding to formulae (4a) and (4b) resp. is not simple, either.

5.2. Mapping of the closed-loop plane $M(s)$ onto the inverse open-loop plane $B(s)$

The mapping $B(s) [M(s)]$ is given by formula (8). To plot the complete chart $(B, \psi, x, y) [M, a, U, V]$ (Fig. 6), following equations may be adopted:

$$\left[(x + 1) - \frac{1}{2U} \right]^2 + y^2 = \left(\frac{1}{2U} \right)^2 \tag{8a}$$

$$(x + 1)^2 + \left[y + \frac{1}{2V} \right]^2 = \left(\frac{1}{2V} \right)^2 \tag{8b}$$

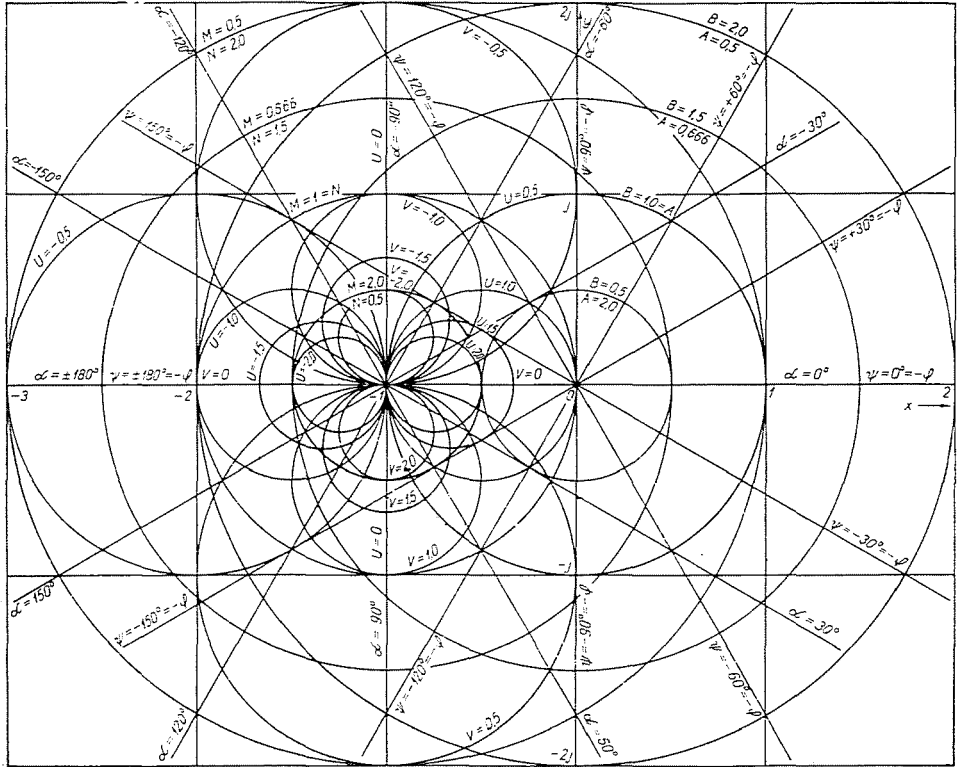


Fig. 6. Mapping of plane $M(s)$ onto the reference plane $B(s)$. Chart $(B, \psi, x, y) [M, a, U, V]$

$$(x + 1)^2 + y^2 = \left(\frac{1}{M}\right)^2 \tag{8c}$$

$$x + 1 + \frac{y}{\operatorname{tg} a} = 0 \tag{8d}$$

This is the other most widespread method of representation. Among the incomplete charts these of the type $(x, y) [M, a]$ [3] and of the type $(B, \psi) [M, a]$ [2] used to be applied as a rule. Stability may be judged on the basis of the well-known inverse NYQUIST diagram [2, 3, 4]. Reading the gain margin and the phase margin is not difficult (by the aid of the circle $B = 1$ and of the straight line $\psi = 180^\circ$).

A special advantage of this method of representation is that the condition $\frac{1}{M} = \text{const.}$ determines concentric circles, while the condition $a = \text{const.}$ determines straight lines, consequently M and a may be well read. Evaluation of the peak M_p and of the bandwidth is easy. The division and multiplication, respectively,

prescribed by Eqs. (4a) and (4b), respectively, may simply be realized by the aid of circles $\frac{1}{M}$ and straights a . Nevertheless, determination of the co-ordinates U and V is somewhat complicated.

5.3. Mapping of the open-loop plane $A(s)$ onto the closed-loop plane $M(s)$

The mapping $M(s)$ [$A(s)$] is expressed by formula (9). The complete chart (M, a, U, V) [A, φ, X, Y] may be seen in Fig. 7, and for the plotting, following equations may be applied:

$$\left[(U - 1) - \frac{1}{2(X + 1)} \right]^2 + V^2 = \frac{1}{2(X + 1)} \tag{9a}$$

$$(U - 1)^2 + \left(V - \frac{1}{2Y} \right)^2 = \left(\frac{1}{2Y} \right)^2 \tag{9b}$$

$$\left(U - \frac{A^2}{A^2 - 1} \right)^2 + V^2 = \left(\frac{A}{A^2 - 1} \right)^2 \tag{9c}$$

$$\left(U - \frac{1}{2} \right)^2 + \left(V + \frac{1}{2 \operatorname{tg} \varphi} \right)^2 = \left(\sqrt{\frac{1}{4} + \frac{1}{4 \operatorname{tg}^2 \varphi}} \right)^2 \tag{9d}$$

Adoption of the incomplete chart (M, a, U, V) [X, Y] belonging to this conformal mapping group has been suggested only recently [11]. The complete chart to be found in Fig. 7 appears here — to our knowledge — for the first time. For those who give preference to the polar form of $A(j\omega)$ over the canonical one, adoption of the incomplete chart (M, a, U, V) [A, φ] may be suggested instead of the chart proposed in [11].

It is important that the closed-loop response $M(j\omega)$ manifests itself directly, if the open-loop response $A(j\omega)$ is plotted onto the plane $M(s)$, whether by the aid of co-ordinates X, Y or A, φ .

This way of representation makes use of the plane $M(s)$ advantageously, consequently $M, a = \text{const.}$ determines the well-known polar co-ordinate system, while $U, V = \text{const.}$ the well-known Cartesian one. For establishing the time function, the data of the real and imaginary frequency response $U(\omega)$ and $V(\omega)$, respectively, may simply be read. Evaluation of the peak M_p and the bandwidth is also easy. The advantages are obvious, when adopting the formulae (4a) and (4b), as in the polar co-ordinate system the division and multiplication is simple.

The disadvantage of this method of representation is, however, that both the set of curves X, Y and the set of curves A, φ are condensed in certain places and are thin in other ones, consequently, plotting $M(j\omega)$ from the data of $A(j\omega)$ is not quite easy.

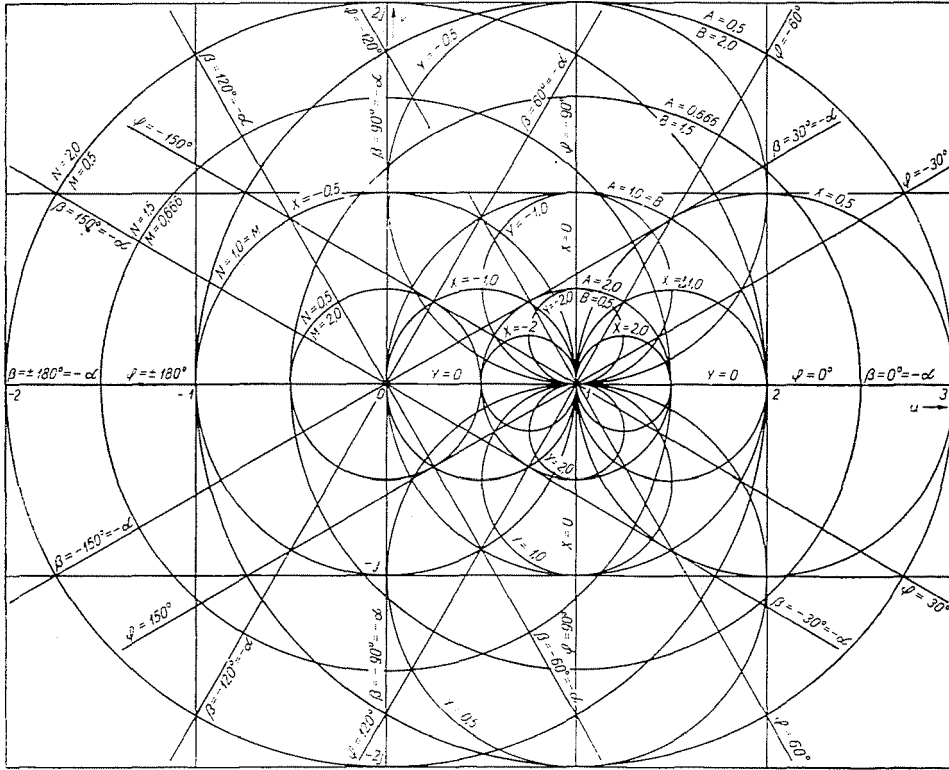


Fig. 8. Mapping of plane $A(s)$ onto the reference plane $N(s)$. Chart $(N, \beta, u, v) [A, \varphi, X, Y]$

the denominator and in the numerator of $M(s)$ (after removing the fractions in the denominator and in the numerator), while the frequency ω increases from 0 to $+\infty$.

5.4. Mapping of the open-loop plane $A(s)$ onto the inverse closed-loop plane $N(s)$

The mapping $N(s) [A(s)]$ is described by formula (10). For plotting the complete chart $(N, \beta, u, v) [A, \varphi, X, Y]$ (Fig. 8), the following equations serve

$$\left[(u - 1) - \frac{1}{2X} \right]^2 + v^2 = \left(\frac{1}{2X} \right)^2 \tag{10a}$$

$$(u - 1)^2 + \left[v + \frac{1}{2Y} \right]^2 = \left(\frac{1}{2Y} \right)^2 \tag{10b}$$

$$(u - 1)^2 + v^2 = \left(\frac{1}{A} \right)^2 \tag{10c}$$

$$u - 1 + \frac{v}{\operatorname{tg} \varphi} = 0. \quad (10d)$$

Transferring the open-loop response $A(j\omega)$ onto the $N(s)$ plane, either on the basis of the co-ordinates A, φ or X, Y , the inverse closed-loop response $N(j\omega)$ is obtained. The curve $N(j\omega)$ may relatively simply be plotted from the polar coordinates of $A(j\omega)$. Also the multiplication and division may easily be performed in the plane $N(s)$. The data of M can readily be obtained from the data of N as they are reciprocal ones. Opposite to these advantages, it is inconvenient, that now $U(\omega)$ and $V(\omega)$ cannot directly be read.

Determination of the open-loop phase margin using circle $A = 1$ is very simple, but to obtain the gain margin, the close circles $X = \text{const.}$ must be applied.

The stability criterion is similar to that of the previous case, nevertheless, curve $N(j\omega)$ must sweep through the quadrants in a positive, counter-clockwise direction, while the frequency ω increases from 0 to $+\infty$. (MIKHAILOV's and LEONHARD's criterion [7, 8, 9, 10].)

5.5. Mapping of the inverse open-loop plane $B(s)$ onto the closed-loop plane $M(s)$

As a following possibility the complete chart $(M, a, U, V) [B, \psi, x, y]$ (Fig. 9) belonging to the conformal mapping $M(s) [B(s)]$ will be examined. For the plotting, the following formulae may be adopted:

$$\left[U - \frac{1}{2(x+1)} \right]^2 + V^2 = \left[\frac{1}{2(x+1)} \right]^2 \quad (12a)$$

$$U^2 + \left(V + \frac{1}{2y} \right)^2 = \left(\frac{1}{2y} \right)^2 \quad (12b)$$

$$\left(U + \frac{1}{B^2 - 1} \right)^2 + V^2 = \left(\frac{B}{B^2 - 1} \right)^2 \quad (12c)$$

$$\left(U - \frac{1}{2} \right)^2 + \left(V - \frac{1}{2 \operatorname{tg} \psi} \right)^2 = \left(\sqrt{\frac{1}{4} + \frac{1}{4 \operatorname{tg}^2 \psi}} \right)^2 \quad (12d)$$

The chart $(M, a, U, V) [B, \psi, x, y]$ was plotted only for the sake of completeness, but it will not be discussed in details, offering the same results, as chart $(M, a, U, V) [A, \varphi, X, Y]$ and being in no respect more advantageous, than it.

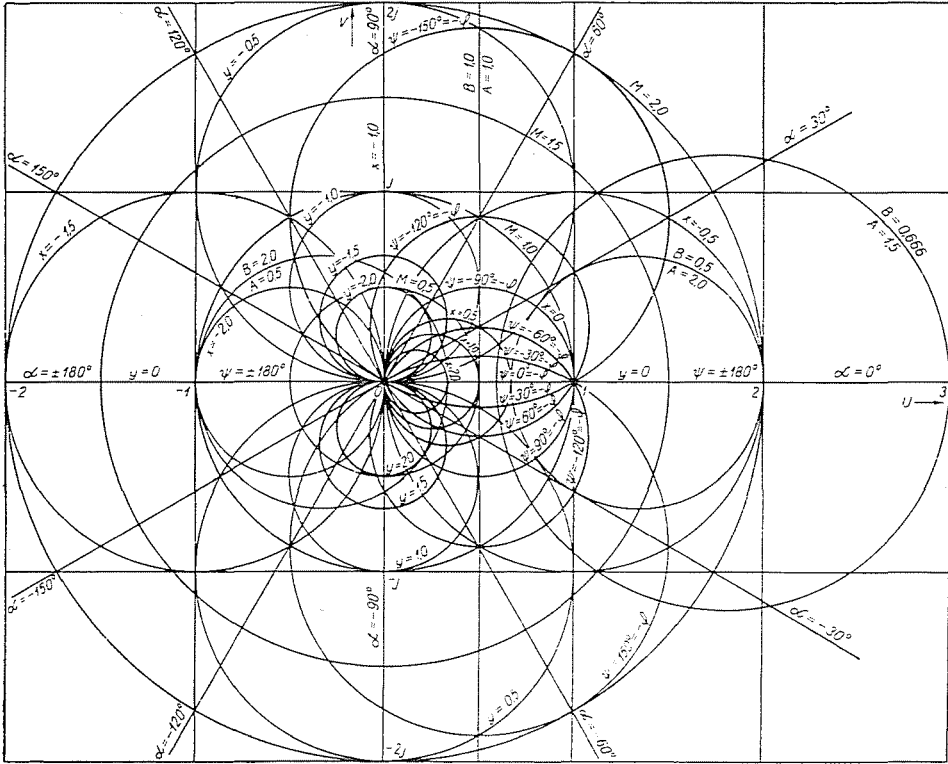


Fig. 9. Mapping of plane $B(s)$ onto the reference plane $M(s)$. Chart (M, α, U, V) $[B, \psi, x, y]$

5.6. Mapping of the inverse open-loop plane $B(s)$ onto the inverse closed-loop plane $M(s)$ and vice versa

The mappings $N(s) [B(s)]$ and $B(s) [N(s)]$ given by formulae (11) and (13), respectively, have exactly the same complete charts

$$(N, \beta, u, v) [B, \psi, x, y] \text{ and } (B, \psi, x, y) [N, \beta, u, v]$$

as a result (Fig. 10). For plotting it, the following formulae may be adopted:

$$u = x + 1 \tag{11a}$$

$$v = y \tag{11b}$$

$$(u - 1)^2 + v^2 = B^2 \tag{11c}$$

$$u - 1 - \frac{v}{\operatorname{tg} \psi} = 0 \tag{11d}$$

or

$$x = u - 1 \tag{13a}$$

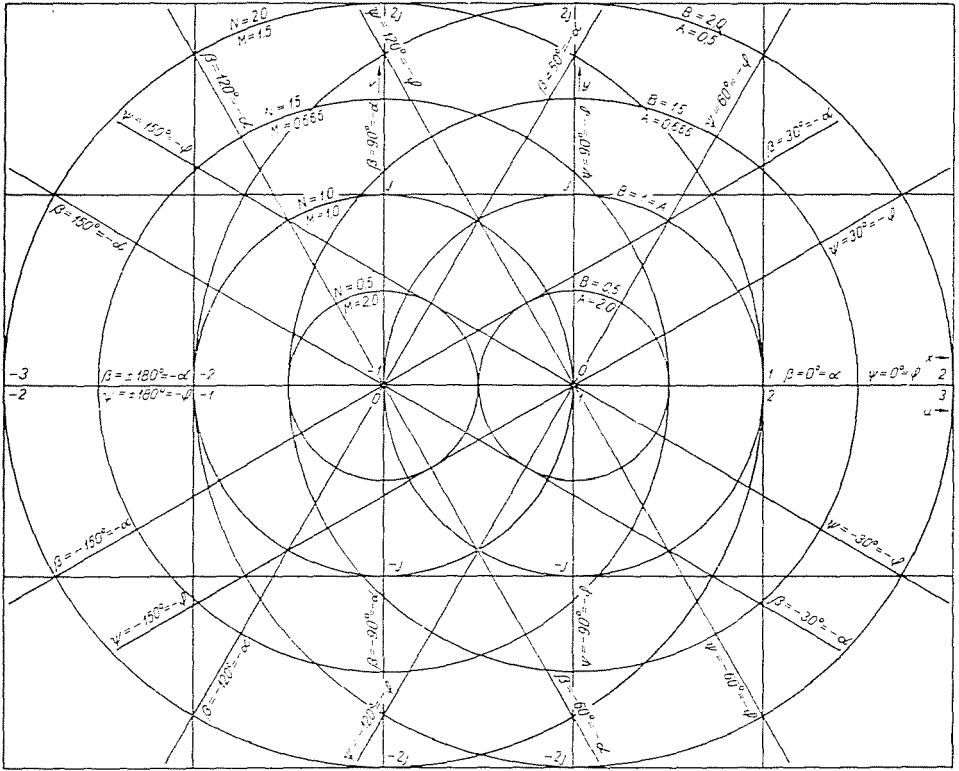


Fig. 10. Mutual mapping of planes $B(s)$ and $N(s)$. Charts (N, β, u, v) [B, ψ, x, y] and (B, ψ, x, y) [N, β, u, v]

$$y = v \tag{13b}$$

$$(x + 1)^2 + y^2 = N^2 \tag{13c}$$

$$x + 1 - \frac{y}{\operatorname{tg} \beta} = 0 \tag{13d}$$

This method of representation has great advantages: among the eight figuring co-ordinates six are determined by parallel equidistant straight lines while two of them by concentric circles. Reading any of the eight co-ordinates is consequently very simple and accurate. The multiplication division may be performed easily by the aid of the polar co-ordinates both in plane $N(s)$ and in plane $B(s)$.

The fact may be regarded as a disadvantage that for obtaining the time functions $U(\omega)$ and $V(\omega)$ cannot be read directly, nevertheless this limitation is not very important as $U(\omega)$ and $V(\omega)$ may be determined by simple formulae on the basis of the polar co-ordinates ($U = \frac{1}{N} \cos \beta$, $V = -\frac{1}{N} \sin \beta$).

It may be regarded as advantageous that a single curve provides simultaneously the inverse closed-loop frequency response $N(j\omega)$ [in the plane $N(s)$] and the inverse open-loop frequency response $B(j\omega)$ [in the plane $B(s)$].

As stability criterion in the plane $B(s)$ the inverse NYQUIST criterion, while in plane $N(s)$ the MIKHAILOV—LEONHARD criterion may be adopted. So from a didactical point of view this method of representation clearly shows the mutual relation between the above-mentioned stability criteria.

The phase margin, gain margin, the peak magnitude, as well as the bandwidth may be easily and accurately read, too.

5.7. Mapping of the inverse closed-loop plane $N(s)$
onto the open-loop plane $A(s)$

The mapping $A(s)$ [$N(s)$] given by Eq. (14) yields the following equations:

$$\left[X - \frac{1}{2(u-1)} \right]^2 + Y^2 = \left[\frac{1}{2(u-1)} \right]^2 \tag{14a}$$

$$X^2 + \left(Y + \frac{1}{2v} \right)^2 = \left(\frac{1}{2v} \right)^2 \tag{14b}$$

$$\left(X - \frac{1}{N^2 - 1} \right)^2 + Y^2 = \left(\frac{N}{N^2 - 1} \right)^2 \tag{14c}$$

$$\left(X + \frac{1}{2} \right)^2 + \left(Y + \frac{1}{2 \operatorname{tg} \beta} \right)^2 = \left(\frac{1}{2 \operatorname{tg} \beta} \right)^2 \tag{14d}$$

These formulae figure, merely for the sake of completeness, and the chart (A, φ, X, X) [N, β, u, v] has not been plotted either, this being in any case less advantageous, than chart (A, φ, X, X) [M, a, U, V].

6. Conclusion

In the foregoing a systematical discussion was given concerning the possibilities of the eight conformal mappings, represented by equations (7)...(14) for plotting the so-called complete charts.

As manifested by the detailed investigation and by Figs. 5...10, besides the generally-used conformal mapping groups $A(s)$ [$M(s)$] and $B(s)$ [$M(s)$] and the recently-suggested incomplete chart (M, a, U, V) [X, Y], the charts furnished by the incomplete chart (M, a, U, V) [A, φ] as well as the conformal mapping group $N(s)$ [$A(s)$] — and perhaps $N(s)$ [$B(s)$] — may be well applied, moreover better, while the charts provided by the conformal mapping group $A(s)$ [$N(s)$] are disadvantageous, consequently their application must be avoided. Especially beneficial seem to be the conformal mappings $N(s)$ [$B(s)$] and

$B(s)$ [$N(s)$], as well as the corresponding charts (N, β, u, v) [B, ψ, x, y] and (B, ψ, x, y) [N, β, u, v], as the mappings in question mean, but a simple displacement, permitting to avoid the inverse formation and the inherent close, or thin circular co-ordinates.

Thus, by the systematic examination realized in the present paper, we succeeded in summarizing all possibilities of plotting the complex-plane charts, pointing out simultaneously the theoretical and practical limitations, the advantages and disadvantages. It is hoped, as concerns the problem investigated, this paper contributes to broadening the horizon of the engineers and experts dealing with control engineering.

Summary

This paper of summarizing and systemizing character sums up and discusses — in our knowledge for the first time — all the possibilities of plotting the complex-plane charts, forming a relation between the closed-loop and open-loop frequency responses. Though theoretically a high number of complex-plane charts differing from each other may be plotted, they all belong to eight conformal mapping groups. Latter provide five practicable methods of representation. By the aid of these charts it can be decided on the basis of the magnitude-phase characteristics, if the closed-loop system stable is and, on the other hand, the design specifications (bandwidth, peak M_p , phase margin, gain margin) may simply be estimated and at the same time the real and imaginary closed-loop frequency response data permitting the determination of the time functions may be simply determined.

References

1. JAMES, H. M.—NICHOLS, N. B.—PHILLIPS, R. S.: Theory of Servomechanisms. McGraw-Hill Book Co. Ltd., New York, London, Toronto, 1947.
2. BROWN, G. S.—CAMPBELL, D. P.: Principles of Servomechanisms. John Wiley & Sons, Inc., New York — Chapman & Hall, Ltd., London, 1948.
3. CHESTNUT, H.—MAYER, R. W.: Servomechanisms and Regulating System Design. John Wiley & Sons, Inc., New York — Chapman & Hall, Ltd., London, 1951.
4. GRABBE, E. M.—RAMO, S.—WOOLDRIGE, D. E.: Handbook of Automation, Computation and Control. Volume I. Control Fundamentals. John Wiley & Sons, Inc., New York — Chapman & Hall, Ltd., London, 1958.
5. BODE, H. W.: Network Analysis and Feedback Amplifier Design. Van Nostrand, Princeton, 1945.
6. NYQUIST, H.: Regeneration Theory. Bell System Techn. Journ., II, 126—147 (1932).
7. Михайлов, А. В.: Метод гармонического анализа в теории регулирования. Автоматика и Телемеханика, Москва, 1938. № 3.
8. Михайлов, А. В.: Теория устойчивости линейных цепей обратной связи с сосредоточенными постоянными. Журнал Технической Физики, Москва, 1939. № 1.
9. LEONHARD, A.: Neues Verfahren zur Stabilitätsuntersuchung. Archiv für Elektrotechnik, **38**, 17—28. (1944).
- 10a. Мееров, М. В.: Основы автоматического регулирования электрических машин. Госэнергоиздат, Москва, 1952.
- 10b. MEJEROW, M. W.: Grundlagen der selbsttätigen Regelung elektrischer Maschinen. VEB Verlag Technik, Berlin, 1954.
11. SHEN, C. F.—SHEN, D. W.: A New Chart Relating Open-Loop and Closed-Loop Frequency Responses of Linear Control Systems. AIEE Transactions, **78**, 252—255, (1959). Part II. Applications and Industry.
- 12a. Солодовников, В. В.: Основы автоматического регулирования. Машгиз, Москва, 1959.
- 12b. SOLODOVNIKOW, W. W.: Grundlagen der selbsttätigen Regelung. Verlag Technik, Berlin, 1959.

Prof. F. CsÁKI, Budapest, XI. Egri J. u. 18. V., Hungary